J|A|C|S
ARTICLES
Published on Web 01/26/2002

Supramolecular Organization of α,α′-Disubstituted Sexithiophenes

A. P. H. J. Schenning,[†] A. F. M. Kilbinger,[§] F. Biscarini,[⊥] M. Cavallini,[||,⊥] H. J. Cooper,[‡] P. J. Derrick,[‡] W. J. Feast,[*,§] R. Lazzaroni,[||] Ph. Leclère,[||] L. A. McDonell,[‡] E. W. Meijer,[*,†] and S. C. J. Meskers[†]

Laboratory of Macromolecular and Organic Chemistry, Eindhoven University of Technology, P.O. Box 513, 5600 MB Eindhoven, The Netherlands, IRC in Polymer Science and Technology, University of Durham, Durham DH1 3LE, U.K., Institute of Mass Spectrometry and Department of Chemistry, University of Warwick, Coventry UK CV4 7AL, U.K., Laboratory for Chemistry of Novel Materials, Center for Research on Molecular Electronics and Photonics, University of Mons-Hainaut, Place du Parc 20, B-7000 Mons, Belgium, and Instituto di Spectroscopia Moleculare, CNR, I-40129 Bologna, Italy

Received May 31, 2001

Abstract: The self-assembly of α,α′-linked sexithiophenes with chiral and achiral penta(ethylene glycol) chains attached at the α- positions of the terminal rings, that is, 2,2′:5′,2″:5″,2‴:5‴,2⁗:5⁗,2⁗′:5⁗′-sexithiophene-5,5⁗′-dicarboxylic acid−(2*S*)-2-methyl-3,6,9,12,15-pentaoxahexadecyl ester (**1**) and 2,2′:5′,2″:5″,2‴:5‴,2⁗:5⁗,2⁗′:5⁗′-sexithiophene-5,5⁗′-dicarboxylic acid−3,6,9,12,15-pentaoxahexadecyl ester (**2**), respectively is described. Analysis of the UV/vis, fluorescence, circular dichroism, and circular polarization of luminescence spectroscopic data shows that these compounds form chiral aggregates in polar solvents and in the solid state. In *n*-butanol aggregation occurs at temperatures below 30 °C, while above this threshold temperature the aggregates break up without an intermediate disordered state of aggregation, and the compounds are molecularly dissolved. The "melting temperature" of the aggregates depends on the concentration of sexithiophene, indicating that the optical changes observed are a result of intermolecular processes. Mass spectrometric measurements reveal that **1** and **2** can form mixed aggregates. Analysis of the optical spectra reveals that in these mixed aggregates, chiral **1** molecules act as "sergeants" to direct the packing of the "soldiers" **2**, illustrating cooperativity within the columns. In water, the same type of chiral aggregates are formed as in *n*-butanol below 30 °C; however, these aggregates are still present, but the chirality is lost above 30 °C. In spin-coated films of **1** chiral aggregates are present. AFM studies show that **1** self-organizes into chiral fiberlike structures in the solid state. Furthermore both **1** and **2** display thermotropic liquid crystalline behavior between 180 and 200 °C.

Introduction

Mesoscopic order in π-conjugated systems is a topic of great importance because it determines the performance of the materials when used as components of organic electrooptical devices such as solar cells,[1] light-emitting diodes (LEDs),[2] and field-effect transistors (FETs).[3,4] Well-defined π-conjugated oligomers can play an important role in this field because their precise chemical structure and conjugation length give rise to defined functional properties and facilitate control over their supramolecular organization.[5] Until recently research in this field has been focused mainly on methodologies for the synthesis and characterization of π-conjugated oligomers with long axis dimensions up to 10 nm.[6,7] In the immediate future, it is expected that interest will focus on the control of the spatial orientation and packing of oligomers through the design of molecular and supramolecular architectures.

Gaining knowledge of the conformations of folded polymers, oligomers, and supramolecular assemblies in solution is of great importance and might lead to improved design of new electroactive materials. It is known that assemblies can exist in a

* To whom correspondence should be addressed.
[†] Laboratory of Macromolecular and Organic Chemistry, Eindhoven University of Technology, P.O. Box 513, 5600 MB Eindhoven, The Netherlands.
[§] IRC in Polymer Science and Technology, University of Durham, Durham DH1 3LE, U.K.
[‡] Institute of Mass Spectrometry and Department of Chemistry, University of Warwick, Coventry UK CV4 7AL, U.K.
[||] Laboratory for Chemistry of Novel Materials, Center for Research on Molecular Electronics and Photonics, University of Mons-Hainaut, Place du Parc 20, B-7000 Mons, Belgium.
[⊥] Instituto di Spectroscopia Moleculare, CNR, I-40129 Bologna, Italy.

(1) (a) Sariciftci, N. S.; Smilowitz, L.; Heeger, A. J.; Wudl, F. *Science* **1992**, *258*, 1474. (b) Yu, G.; Gao, J.; Hummelen, J. C.; Wudl, F.; Heeger, A. J. *Science* **1995**, *270*, 1789. (c) Halls, J. J. M.; Walsh, C. A.; Greenham, N. C.; Marseglia, E. A.; Friend, R. H. *Nature* **1995**, *376*, 498.
(2) Bourroughes, J. H.; Bradley, D. D. C.; Brown, A. R.; Marks, R. N.; MacKay, K.; Friend, R. H.; Burn, P. L.; Holmes, A. B. *Nature* **1990**, *347*, 539.
(3) Brown, A. R.; Pomp, A.; Hart, C. M.; de Leeuw, D. M. *Science* **1995**, *270*, 972.
(4) Sirringhaus, H.; Tessler, N.; Friend, R. H. *Science* **1998**, *280*, 1741.
(5) Martin, R. E.; Diederich, F. *Angew. Chem., Int. Ed.* **1999**, *38*, 1350.
(6) Tour, J. M. *Chem. Rev.* **1996**, *96*, 537.
(7) Fichou, D. *J. Mater. Chem.* **2000**, *10*, 571.

Scheme 1

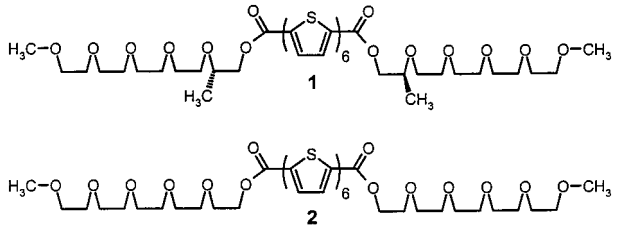

disordered collapsed state, in a unique structure with a well-defined conformation, or in a disordered intermediate state that is present between the well-defined folded structure or aggregate and the unfolded or disassembled state.[8] For assemblies in protic solvents detailed information concerning conformational uniqueness is scarce.[9] Recently, the folding process of a series of oligo(*m*-phenylene ethynylene)s has been studied, in which first a disordered state is formed before a unique helical conformation is obtained.[10] Such a two-step phase transition was also found in self-assembled C_3-symmetrical disk-shaped molecules in *n*-butanol.[11] Upon increasing the temperature chiral columns first form columns lacking supramolecular chirality and then molecularly dissolve. The introduction of a stereocenter into the side chain was shown to provide a very informative probe in studying the expression of chirality at the supramolecular level.[12]

Oligomers and polymers based on α,α′-linked thiophenes are at the forefront of organic semiconductor materials with potential for applications in FETs and related structures. In particular α,α′-linked sexithiophenes (α-6T) have been shown to have desirable properties which are highly dependent on the supramolecular morphology adopted.[7] Polymer studies of the solution organization of chirally *β*-substituted polythiophenes gave profound insights into the solid-state organization of solution-cast films.[13] There have been several attempts to solubilize sexithiophenes by substitution at the terminal α-positions,[14] but the supramolecular organization of the materials in solution has not been described. Here we report results concerning the structural organization of sexithiophenes carrying respectively chiral (2*S*)-2-methyl-3,6,9,12,15-pentaoxahexadecyl (**1**) and 3,6,9,12,15-pentaoxahexadecyl (**2**) esters at both the terminal α positions of the sexithiophene unit, (Scheme 1).

Results and Discussion

Synthesis and Characterization. We reported the synthesis of the chiral 2,2′:5′,2″:5″,2‴:5‴,2⁗:5⁗,2⁗′:5⁗′-sexithiophene-5,5⁗′-di-carboxylic acid (2*S*)-2-methyl-3,6,9,12,15-pentaoxahexadecyl ester **1**, previously.[15] Achiral 2,2′:5′,2″:5″,2‴:5‴,2⁗:5⁗,2⁗′:5⁗′,2⁗′′-sexithiophene-5,5⁗′′-dicarboxylic acid−3,6,9,12,15-pentaoxahexadecyl ester **2** was synthesized by an analogous route in which (2*S*)-2-methyl-3,6,9,12,15-pentaoxahexadecanol,[11] was replaced by 3,6,9,12,15-pentaoxahexadecanol.[16]

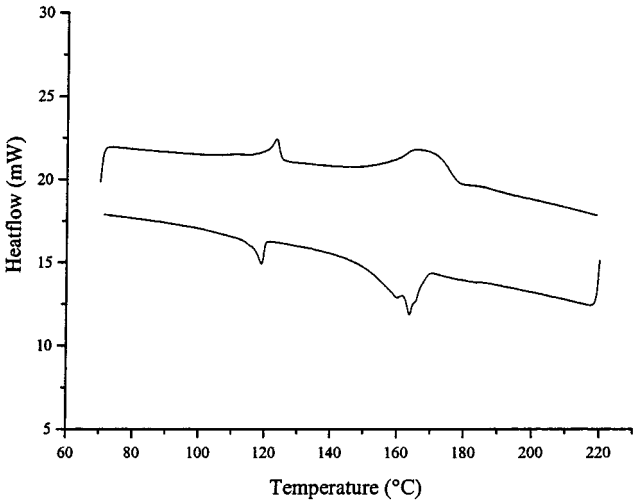

Figure 1. DSC traces of **1**.

1 and **2** showed thermotropic liquid crystalline behavior in a relative small temperature range. Thermal analysis using DSC showed, in the case of **1**, an exothermic transition at 120 °C, a complex multiple transitions at 165−175 °C and a small transition at 180 °C (Figure 1). Polarized optical microscopy revealed that the first transition is due to a crystal−crystal transition. Furthermore, the texture observed at 180 °C is reminiscent of a smectic C phase, and at 190 °C, of a smectic A phase (Figure 2). Above 200 °C the compound forms an isotropic melt. DSC traces of **2** revealed an exothermic transition at 40 °C and a complicated set of transitions between at 180 and 195 °C. The first transition at 40 °C is again a crystal−crystal transition, while between 180 and 195 °C the same type of textures are observed as for **1**.

Self-Assembly and Solvatochromism. The UV/vis absorption spectra of **1** and **2** in THF are identical with the strongest band located at $\lambda_{max} = 452$ nm while weaker bands are visible at higher energies (Figure 3 shows the data recorded for **2**). These spectra are typical for molecularly dissolved α,α′-terminally disubstituted sexithiophene chromophores.[14] The fluorescence spectrum has a maximum at 528 nm and shows characteristic vibronic fine structure, while the observed high intensity provides further evidence that the material is molecularly dissolved The absence of aggregation is also supported by the absence of a CD signal in the case of **1** in this solvent.

A solution of **1** in *n*-butanol at 20 °C shows a UV/vis absorption spectrum typical for aggregated sexithiophene derivatives[17] with a main band at $\lambda_{max} = 403$ nm blue-shifted by $\Delta\lambda = \sim 50$ nm compared to a chloroform or THF solution in

(8) (a) Lokey, R. S.; Iverson, B. L. *Nature* **1995**, *375*, 303. (b) Gellman, S. H. *Acc. Chem. Res.* **1998**, *31*, 173. (c) Seebach, D.; Matthew, J. L. *Chem. Commun*. **1997**, 2015. (d) Nelson, J. C.; Saven, J. G.; Moore, J. S.; Wolynes, P. G. *Science* **1997**, *277*, 1793.
(9) For a recent review, see: Lydon J. *Curr. Opin. Colloid Interface Sci.* **1998**, *3*, 458.
(10) Prince, R. B.; Brunsveld, L.; Meijer, E. W.; Moore, J. S. *Angew. Chem., Int. Ed.* **2000**, *39*, 228.
(11) Brunsveld, L.; Zhang, H.; Glasbeek, M.; Vekemans, J. A. J. M.; Meijer, E. W. *J. Am. Chem. Soc.* **2000**, *122*, 6175.
(12) See also: (a) Palmans, A. R. A.; Vekemans, J. A. J. M.; Havinga, E. E.; Meijer, E. W. *Angew. Chem., Int. Ed. Engl.* **1997**, *36*, 2648. (b) Sandström, J. In *Circular Dichroism: Principles and Applications*; Nakanishi, K., Berova, N., Woodey, R., Eds.; VCH: Weinheim, 1994.
(13) Meskers, S. C. J.; Peeters, E.; Langeveld-Voss, B. M. W.; Janssen, R. A. J. *Adv. Mater*. **2000**, *12*, 589.
(14) (a) Bäuerle, P. In *Electronic Materials: The Oligomer Approach*; Müllen, K., Wegner, G., Eds; VCH: Weinheim, 1998. (b) Katz, H. E.; Dodabalapur, A.; Torsi, L.; Elder, D. *Chem. Mater*. **1995**, *7*, 2238. (c) Katz, H. E. *J. Mater. Chem.* **1997**, *7*, 369. (d) Katz, H. E.; Laquindanum, J. G.; Lovinger, A. J. *Chem. Mater.* **1998**, *10*, 633. (e) Garnier, F.; Yassar, A.; Hajlaoui, R.; Horowitz, G.; Deloffre, F.; Servet, B.; Ries, S.; Alnot, P. *J. Am. Chem. Soc.* **1993**, *115*, 8716. (f) Parakka, J. P.; Cava, M. P. *Tetrahedron* **1995**, *51*, 2229.
(15) Kilbinger, A. F. M.; Schenning, A. P. H. J.; Goldoni, F.; Feast, W. J.; Meijer, E. W. *J. Am. Chem. Soc.* **2000**, *122*, 1820.
(16) Brunsveld, L.; Lohmeijer, B.; Vekemans, J. A. J. M.; Meijer, E. W. *Chirality* **2002**. In press.
(17) For a solid-state spectrum of α-6T, see: (a) Yassar, A.; Horowitz, G.; Valat, P.; Wintgens, V.; Hmyene, M.; Deloffre, F.; Srivastava, P.; Lang, P.; Garnier, F. *J. Phys. Chem.* **1995**, *99*, 9155. (b) Muccini, M.; Lunedei, E.; Taliani, C.; Beljonne, D.; Cornil, J.; Brédas, J. L. *J. Chem. Phys.* **1998**, *109*, 10513.

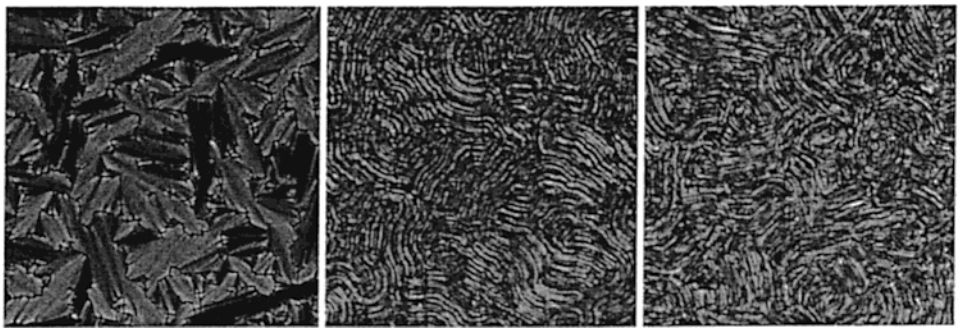

Figure 2. Texture of **1** at 160 (right), 170 (middle) and 180 °C (left) obtained by polarized optical microscopy.

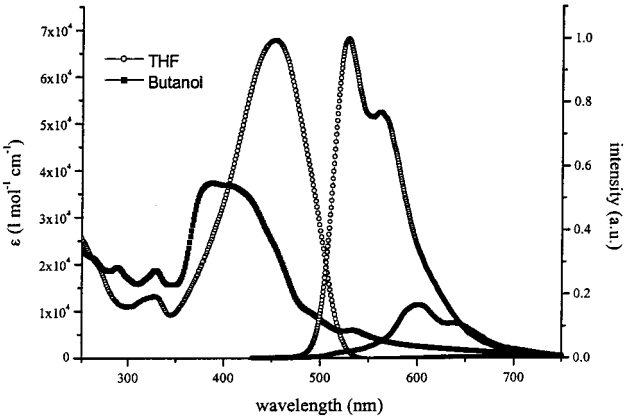

Figure 3. UV−vis (left) and fluorescence (right) spectra of **2** in THF and butanol.

which the compound is molecularly dissolved. In the case of solutions of **2** in *n*-butanol an even larger blue-shift was observed, $\Delta\lambda = 71$ nm, $\lambda_{max} = 381$ nm (Figure 3). The fluorescence intensity of solutions of both compounds in *n*-butanol was reduced when compared to chloroform solutions, and the λ_{max} was located at 600 nm. A bisignate CD effect was observed for **1** in *n*-butanol (Figure 4a), exhibiting a negative Cotton effect at lower and a positive Cotton effect at higher energy ($\lambda = 376$ nm). The zero crossing is within 5 nm of the absorption maximum of the chromophore, indicating strong exciton coupling in the sexithiophene aggregates.[12] Circular polarization of the fluorescence of **1** in *n*-butanol could also be observed. A maximum dissymmetry factor (g_{lum}) of $-2.2 \pm 0.2 \times 10^{-3}$ at $\lambda = 650$ nm was found for which the sign is in agreement with the sign of the CD at lowest energy.[18] Hence, a well-defined chiral aggregate of **1** is formed in *n*-butanol, that not only possesses a chiral ground state, but the excited state is chiral as well, indicating that the chirality is the result of supramolecular ordering. The larger blue-shift in the UV/vis spectrum found for aggregates of **2** in solution could indicate that these structures are better packed, resulting in a stronger exciton coupling.[19] In this case if the aggregate is a helical stack, a racemic mixture of both left- and right-handed helical aggregates must be formed.

Compounds **1** and **2** also show aggregation in water at room temperature. Both UV/vis absorption spectra are similar to those of *n*-butanol solutions at 20 °C with the main band at $\lambda_{max} = 406$ nm for **1** and $\lambda_{max} = 381$ nm for **2**. The fluorescence maximum is red-shifted (600 nm) with respect to that observed in THF solution, and the intensity is reduced, indicating aggregation. A bisignate CD effect was observed for **1** in water, exhibiting a negative Cotton effect at lower and a positive Cotton effect at higher energy. Circular polarization of the luminescence was observed with a maximum dissymmetry factor (g_{lum}) of $-4.8 \pm 0.5 \times 10^{-3}$, which is in agreement with the sign of the CD at lowest energy.

When an apolar solvent such as hexane was used, the same type of absorption spectrum was found, indicating that in this solvent the same type of aggregates are formed. Taken together, these data indicate that the variation between molecular dissolution and aggregation in solution is a subtle function of solvent polarity: aggregation occurring in nonpolar and polar solvents, and molecular dissolution in slightly polar solvents.

Self-Assembly and Thermochromism. The temperature dependence of the aggregation process was studied in the range −10 to 80 °C, using UV/vis absorption, CD, and fluorescence spectroscopy. Initially solutions were cooled to −10 °C and then warmed to 80 °C slowly and stepwise with 10 min allowed for equilibration of the sample at each recording temperature. In butanol solutions below 20 °C the UV/vis, CD, and fluorescence spectra of **1** are typical of aggregated sexithiophenes, while above 40 °C the spectrum of the molecularly dissolved species is obtained (Figure 4). The phase transition is fully reversible, as a subsequent cooling run gave identical spectra.[20] In the case of spectra for solutions of **2** recorded at same concentration, thermochromic behavior similar to that observed for **1** is found, but the "melting transition"[21] occurs at a higher temperature.[22] For aqueous solutions of **1**, on the other hand, only the CD signal is lost above 40 °C (Figure 5), while UV/vis and fluorescence spectra indicate that the compound remains in its aggregated form. The CD signal for **1** in water goes through zero near the absorption maximum of the chromophore for spectra recorded at 40 °C and above (Figure 5). The shape of the CD trace in water and *n*-butanol is quite similar above 40 °C, indicating that presumably the same type of aggregate is formed. Below 40 °C the shape of the CD spectrum changes, possibly indicating a small reorganization of the aggregates.

(18) Langeveld-Voss, B. M. W.; Beljonne, D.; Shuai, Z.; Janssen, R. A. J.; Meskers, S. C. J.; Meijer, E. W.; Brédas, J. L. *Adv. Mater.* **1998**, *10*, 1343.
(19) McRea, E. G.; Kasha, M. *J. Phys. Chem.* **1958**, *28*, 721.
(20) Further evidence of this temperature-dependent reversible aggregation of **1** in deuterated *n*-butanol was obtained from the NMR spectra of 12 mM solution; broad lines were observed below 90 °C, and sharp ones, above.
(21) While melting is strictly concerned with the crystal-to-liquid state transition we adopt the practice of the biological sciences in referring to the disruption of highly organized aggregates in fluid media as melting, see: Saenger, W. *Principles of Nucleic Acid Struture*; Springer-Verlag: New York Inc., 1984; p 143.
(22) The "melting temperature" was found to be concentration-dependent. For example, at a concentration of 2.6×10^{-6} M of **1** in butanol, the temperature was $T_m = 9$ °C, while at a concentration of 6.0×10^{-5} M this value was $T_m = 33$ °C.

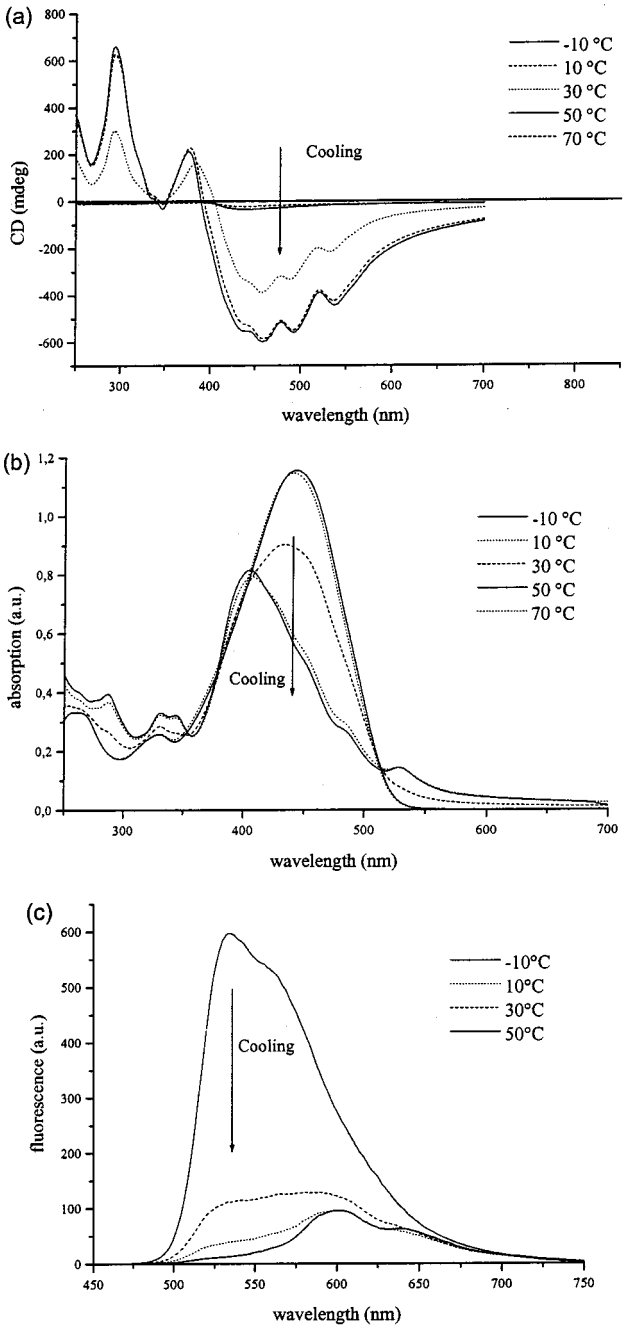

Figure 4. Temperature-dependent CD (a), UV/vis (b), and fluorescence (c) spectra of **1** in *n*-butanol (2.6×10^{-5} mol·L^{-1}).

When the normalized aggregate/monomer ratio taken from the spectral maxima is plotted against temperature a sharp transition is observed (Figure 6). The sigmoidal curves obtained could be fitted with a Boltzmann distribution

$$\alpha = \frac{1}{1 + e^{(T-T_m)/\Delta T}} \qquad (1)$$

in which α is the fraction of aggregated molecules, T_m is the "melting temperature" at which $\alpha = 0.5$, and ΔT relates to the width of the transition.[23] In the case of **1** in butanol, using the same concentrations in the UV/vis, CD, and fluorescence

(23) Apperloo, J. J.; Janssen, R. A. J.; Malenfant, P. R. L.; Fréchet J. M. J. *Macromolecules* **2000**, *33*, 7038.

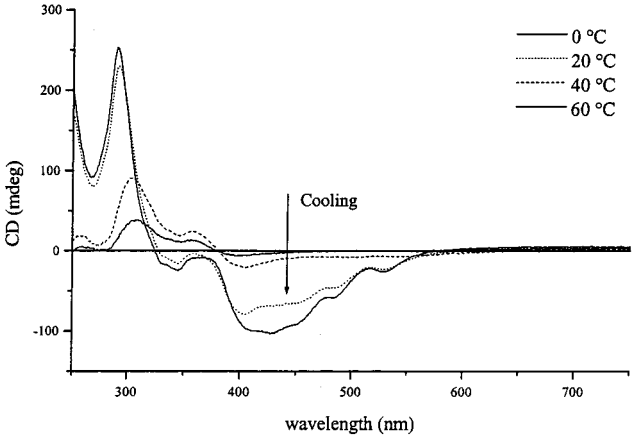

Figure 5. Temperature-dependent CD spectra of **1** in water (2.6×10^{-5} mol·L^{-1}).

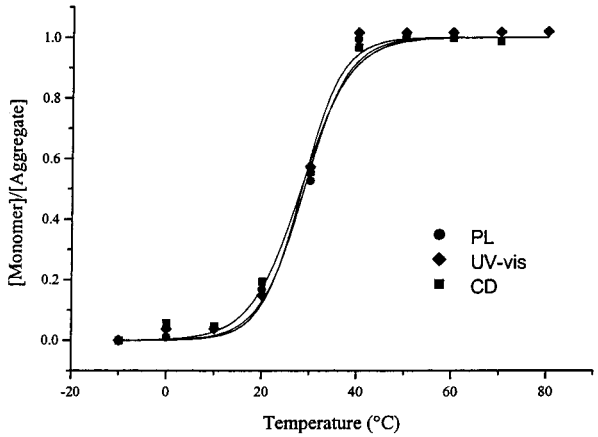

Figure 6. Normalized aggregate/monomer ratio versus temperature of **1** in *n*-butanol (2.6×10^{-5} mol·L^{-1}) and the fitted curves.

experiments, similar melting temperatures were found {T_m = 28.3 °C (CD), T_m = 28.1 °C (UV−vis), T_m = 28.8 °C (fluorescence)}. As can be concluded from the fitted curve, the aggregation occurs in a temperature range of approximately 20 °C, which points to a strongly cooperative process.[11] The three techniques prove the existence of two phases in *n*-butanol solution, that is, aggregates at low temperature and molecularly dissolved species at high temperature. These combined results show unambiguously that chiral aggregates are breaking up or are formed directly without an intermediate disordered aggregated state. In the case of **2** a higher "melting temperature" in *n*-butanol was found (T_m = 48.3 °C). This difference is probably due to the absence of a branched unit in the oligo(ethylene oxide) side chain of **2**, resulting in a better packing and stronger aggregation.

The CD measurement of **1** in water shows a melting transition at T_m = 34 °C while UV/vis and fluorescence do not show any transition. This corresponds to a transition from chiral helical aggregates to achiral disordered aggregates in which the side chains are more mobile and cannot induce chiral information in the sexithiophene stack.

"Sergeant and Soldiers". Chirality in aggregates can arise from the presence of only a small proportion of chiral molecules in an assembly of largely achiral molecules; the phenomenon is generally known as the "sergeant and soldiers" effect.[24] Chiral **1** was tested as the potential "sergeant" to direct the packing of

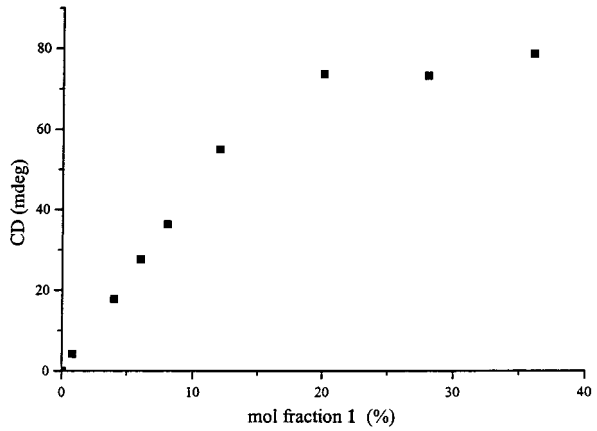

Figure 7. Cotton effect (mdeg) as function of the mol fraction of "sergeant" **1** compared to "soldier" **2**.

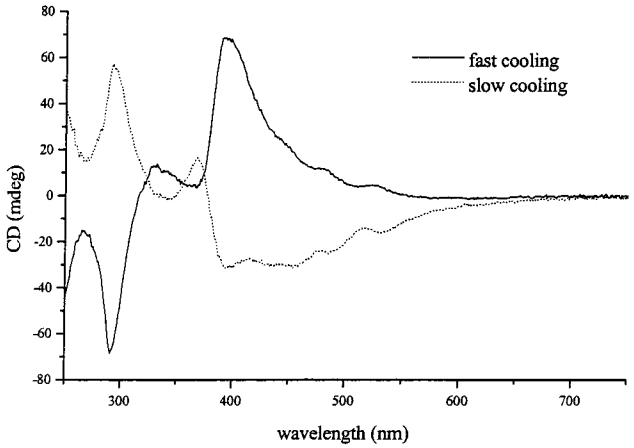

Figure 8. Cotton effect observed after fast and slow cooling of a mixture of **1** and **2**.

the "soldiers", i.e., achiral **2**. However, mixing a small amount of **1** in *n*-butanol solution of **2** did not result in amplification of the CD effect. A linear relation was observed between the mol fraction of **1** and the CD effect, indicating that there was no exchange between the aggregates of **2** and **1** under these conditions. Amplification of the chirality was only found when the samples were heated above the aggregate "melting temperature" and then slowly cooled (Figure 7). After addition of 30 mol % of "sergeant" molecules, all stacks had gained the same chirality as stacks exclusively formed from "sergeant" **1**. Although the percentage of sergeants used is relatively high, this result illustrates that the "sergeant and soldiers" phenomenon operates in protic media.[25] However, the rate of cooling is crucial. When mixtures of **1** and **2** in the molecular ratio 1:3 were cooled slowly, a CD spectrum similar to that of pure **1** was found. On the other hand fast cooling produced a CD spectrum which was the inverse of the one obtained by slow cooling (Figure 8). This phenomenon has been observed previously for low-molecular weight organic compounds and polymers in the solid state.[26] Slow cooling gives the thermodynamically most stable form of the mixed aggregate, while fast cooling gives the kinetically favored form. It is interesting to note that the "melting temperature" of **2** is higher than that of chiral **1**, which suggests that aggregates of **2** act as seeds for the aggregating mixtures. Further work is needed to gain a detailed understanding of the remarkable phenomena of mixed ordered aggregate formation, some light being shed by the work described in the next section.

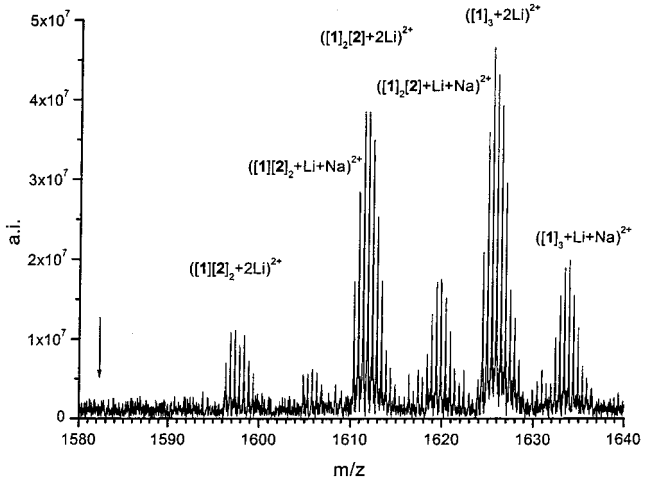

Figure 9. FT-ICR mass spectrum showing the mixed trimer aggregates of **1** and **2** as lithium and sodium ion adducts. The arrow marks the position where the homotrimer of **2** would be expected.

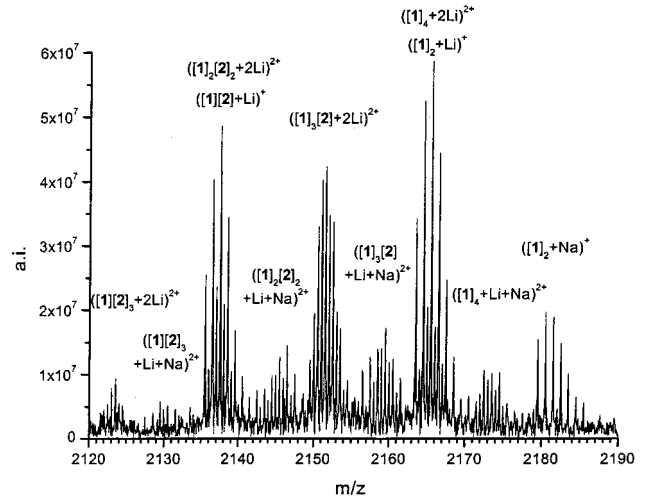

Figure 10. FT-ICR mass spectrum showing the mixed tetramer aggregates of **1** and **2** as lithium and sodium ion adducts.

Mass-Spectrometric Evidence for Mixed Aggregation. As previously shown, aggregates of **1** up to the hexamer can be detected by electrospray ionization Fourier transform ion cyclotron resonance mass spectrometry (FT-ICR MS).[27] Nanospray, a variant of electrospray ionization, from an equimolar solution of **1** and **2** in a THF−water mixture, containing LiCl showed peaks corresponding to monomeric compounds **1** and **2** as well as mixed aggregates (dimer, trimer, tetramer, pentamer, and heptamer). By way of illustration, Figure 9 shows the mixed trimers, and Figure 10, the mixed tetramers of **1** and **2** as dilithium and mixed sodium/lithium ion adducts. The mixed pentamer and heptamer aggregates were observed as weak peaks

(24) Green, M. M.; Reidy, M. P.; Johnson, R. D.; Darling, G.; O'Leary, D. J.; Wilson, G. *J. Am. Chem. Soc.* **1989**, *111*, 6452.
(25) Brunsveld, L.; Schenning, A. P. H. J.; Broeren, M. A. C.; Janssen, H. M.; Vekemans, J. A. J. M.; Meijer, E. W. *Chem. Lett.* **2000**, 292.
(26) (a) Lifson, S.; Andreola, C.; Peterson, N. C.; Green, M. M. *J. Am. Chem. Soc.* **1989**, *111*, 8850. (b) Green, M. M.; Sato, T.; Teramoto, A.; Lifson, S. *Macromol. Symp.* **1996**, *101*, 363. (c) Langeveld-Voss, B. M. W.; Waterval, R. J. M.; Janssen, R. A. J.; Meijer, E. W. *Macromolecules* **1999**, *32*, 227.
(27) Kilbinger, A. F. M.; Cooper, H. J.; McDonnell, L. A.; Feast, W. J.; Derrick, P. J.; Schenning, A. P. H. J.; Meijer, E. W. *Chem. Commun.* **2000**, 383.

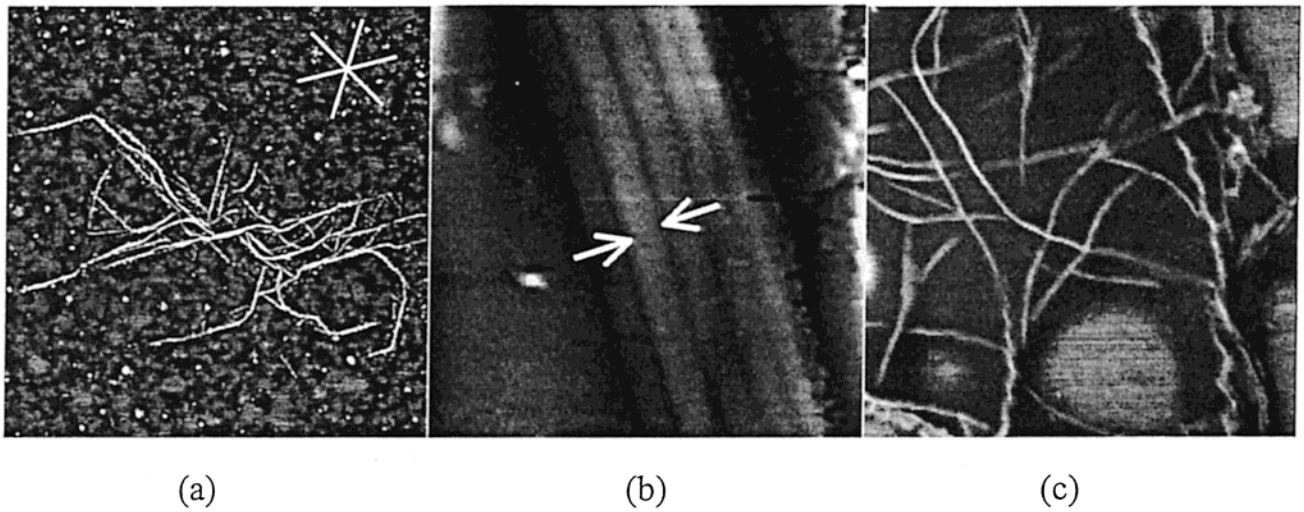

Figure 11. Scanning probe microscopy images of thin deposits cast from 10 μM toluene solutions of **1**. (a) 4.0 × 4.0 μm^2 tapping-mode AFM phase image showing the preferential orientation of large ribbons on graphite. The three-fold symmetry is indicated as a guide; (b) 80 × 80 nm^2 STM topographic image (bias = 1.0 V; current = 0.30 nA) showing the internal structure of a large ribbon on graphite. The white arrows indicate the width of a single thin ribbon. The vertical grayscale is 15 nm; (c) 700 × 700 nm^2 tapping-mode AFM phase image on silicon, showing left-handed helical aggregates.

and are not shown here. The experimental isotope patterns matched the theoretical ones, confirming that each set of peaks represented a single species. The measured mass-to-charge ratios (m/z) agreed with those calculated within 3 ppm in all cases.

It is interesting to note that the mixed aggregates with higher content of **2**, such as $([\mathbf{1}][\mathbf{2}]_2 + 2\mathrm{Li})^{2+}$ (Figure 9) or $([\mathbf{1}][\mathbf{2}]_3 + 2\mathrm{Li})^{2+}$ (Figure 10), show significantly lower intensities in the mass spectrum than the mixed aggregates with a lower content of **2**. While the homotrimer and the homotetramer of **1** show very high intensities, peaks for the analogous homotrimer and -tetramer of **2** were not observed. This can be explained by assuming that **2** forms stronger and consequently larger aggregates than **1**, thereby lowering the effective concentration of **2** in solution as well as the probability of forming mixed aggregates with relatively high content of **2**. In the series of mixed aggregates (dimer to heptamer) the most intense peak moves progressively away from the all-chiral aggregates, that is, **1**, as the aggregates get bigger. This is the sort of pattern one would expect, assuming similar aggregation affinities, if the effective concentration of the achiral species were less.

Solid-State Behavior. To investigate whether a chiral superstructure was formed in the solid state, a drop-cast film of **1** (from THF solution) was prepared and examined spectroscopically. Despite a relatively low absorption at the λ_{max}, an even more intense Cotton effect than the one measured in aqueous solution was observed. The Cotton signal passed through zero near the absorption maximum of the chromophore with a negative Cotton effect at lower energy (408 nm, 3.04 eV, $g_{abs} = -2.42 \times 10^{-2} \pm 0.2 \times 10^{-3}$) and a positive Cotton effect at higher energy (377 nm, 3.29 eV, $g_{abs} = +2.71 \times 10^{-2} \pm 0.2 \times 10^{-3}$). Temperature-dependent measurements showed a transition at 170 °C, and at 200 °C the Cotton effect disappeared. These two temperatures correspond well with the solid−liquid crystalline and liquid crystalline-isotropic melt transitions.

The aggregation process of **1** and **2** in the solid state was further investigated with atomic force microscopy (AFM). Both compounds gave similar results. Figure 11 shows the typical morphology for deposits obtained from a 10 μM toluene solution of **1** and **2**. Toluene was chosen as the solvent because: (i) **1** and **2** do not aggregate in toluene (the behavior is thus similar to that in THF solutions) and (ii) its relatively low evaporation rate at room temperature favors the formation of organized structures.

AFM data previously collected on various conjugated/nonconjugated rod−coil copolymers all show regular arrangements of microfibrillar structures, such as those observed in Figure 11a. This fibrillar morphology appears to be a typical signature of the organization of these conjugated copolymers in the solid state. The fibrils are in fact ribbonlike objects, as their width is much larger than their height (in the image of Figure 11a, the width ranges from 30 to 50 nm, while the height is around 3 nm). Using scanning tunneling microscopy (STM) allows one to image the internal structures of those large ribbons. A typical image is shown in Figure 11b: the large ribbons comprise a few (often five) individual thin ribbons, approximately 7 nm in width. The formation of ribbons, as in the case of other conjugated homopolymers[28] or block copolymers,[29] takes place by self-assembly governed by $\pi-\pi$ stacking of the sexithiophene units. These π-stacks most probably form the core of the thin ribbons, with the ethylene glycol segments located on each side. Interestingly, the dimension estimated for the molecule with the two lateral poly(ethylene glycol) segments fully extended is about 6.8 nm. This suggests that the thin ribbons are one-molecule-wide π-stacks. The length of the ribbons indicates that such π-stacking can extend over hundreds of nanometers, that is, hundreds of molecules (Figure 11a). It is interesting to note that the large ribbons tend to be aligned along three directions at an angle of 120° to each other (Figure 11a). This arrangement is reminiscent of the three-fold symmetry of the graphite surface, indicating that interactions with the substrate can also play an important role in the chain-packing in the solid. When deposits are prepared on the surface of a silicon wafer, thin fibrils are also formed, but they present a helical shape (Figure 11c), which is a clear signature of the

(28) (a) Samorì, P.; Francke, V.; Müllen, K.; Rabe, J. *Chem. Eur. J.* **1999**, *5*, 2312. (b) Samorì, P.; Sikharulidze, I.; Francke, V.; Müllen, K.; Rabe, J. *Nanotechnology* **1999**, *10*, 77.
(29) Leclère, Ph.; Calderone, A.; Marsitzky, D.; Francke, V.; Geerts, Y.; Müllen, K.; Brédas, J. L.; Lazzaroni, R. *Adv. Mater.* **2000**, *12*, 1042.

chirality of the assemblies. Only left-handed helices are observed, and we have checked that **2** forms nonchiral fibrils on the silicon surface. The interplay between molecule−surface interactions and assembly into chiral structures is currently under investigation.

Conclusions

Chiral and achiral sexithiophenes terminally disubstituted at the α-positions with polar tails have been synthesized which form helical aggregates in water, butanol and in the solid state. The "melting transitions" in the two solvents are completely different. In butanol this transition is from helical aggregates to molecularly dissolved species, while in water for **1** a transition from helical aggregates to nonhelical aggregates takes place. The latter transition could only be detected with temperature-dependent circular dichroism, showing the strength of this technique. AFM showed that the molecules self-assemble into helical fibrils with a very large aspect ratio.

Chiral **1** and achiral **2** sexithiophenes form mixed aggregates, and this was directly confirmed by FT-ICR mass spectroscopy. In these mixed aggregates the chiral packing is directed by the chiral sexithiophenes. An interesting inversion of chirality was observed when mixed aggregates were formed by fast (as opposed to slow) cooling. By combining the sergeant and soldiers experiments and the mass spectrometry measurements, we have found the beginnings of an insight into mixed aggregation prior to crystallization. In this process chiral molecule **1** acts as a probe for homocrystallization.

Experimental Section

General Methods. ^{1}H NMR and ^{13}C NMR spectra were recorded at room temperature on a Varian Mercury 400 MHz spectrometer. Chemical shifts are given in ppm (δ) relative to tetramethylsilane. Abbreviations used are s = singlet, d = doublet, t = triplet, q = quartet, and br = broad. Infrared spectra were recorded using a Perkin-Elmer Spectrum One UATR FT-IR spectrophotometer. MALDI-TOF MS spectra were measured on a Perspective DE Voyager spectrometer utilizing a α-cyano-4-hydroxycinnamic acid matrix. GC−MS measurements were performed on a Shimadzu GC/MS-QP5000. Optical spectra were recorded on a Perkin-Elmer Lambda 900 spectrophotometer for UV/vis, a Jasco J-600 spectropolarimeter for CD, a Perkin-Elmer LS50B luminescence spectrometer for fluorescence, and a home-built instrument for circularly polarized luminescence. Temperature-dependent spectra were recorded using a RC 20 Lauda thermo state; during measurements the temperature was kept constant within 0.1 K. Spectra at different temperatures are not corrected for volume changes of the solvent.

5-Bromo-2,2′-bithiophene-5′-carboxylic Acid-3,6,9,12,15-pentaoxahexadecyl Ester. Pentaethylene glycol (2.38 g, 7.8 mmol) was added to a solution of 5-bromo-2,2′-bithiophene-5′-carbonyl chloride (2.38 g, 7.8 mmol) and pyridine (0.6 mL) in toluene (40 mL) and refluxed for 12 h. The solution was poured into water and extracted with diethyl ether (3 × 30 mL); the organic phase was separated and dried ($MgSO_4$). Evaporation of the solvent gave 5-bromo-2,2′-bithiophene-5′-carboxylic acid-3,6,9,12,15-pentaoxahexadecyl ester (2.25 g, 55%) as a yellow oil. ^{1}H NMR (400 MHz, $CDCl_3$) δ 3.30 (s, 3H), 3.47−3.63 (m, 6H), 3.75 (t, J = 4.8 Hz, 2H), 4.36 (t, J = 4.8 Hz, 2H), 6.94 (m, 2H), 7.00 (d, J = 3.8 Hz, 1H), 7.62 (d, J = 3.8 Hz); ^{13}C NMR (100 MHz, $CDCl_3$) δ 58.76, 64.17, 68.84, 70.24, 70.30, 70.33, 70.36, 70.38, 70.47, 71.65 112.69, 123.84, 125.09, 130.74, 131.49, 134.12, 137.45, 142.76, 161.51.

2,2′:5′,2″:5″,2‴:5‴,2⁗:5⁗,2⁗′-Sexithiophene-5,5⁗′-dicarboxylic Acid-3,6,9,12,15-pentaoxahexadecyl Ester (2). A mixture of 5-bromo-2,2′-bithiophene-5′-carboxylic acid-3,6,9,12,15-pentaoxahexadecyl ester (2.25 g, 4.3 mmol), 5,5′-bis(trimethyltin)-2,2′-bithiophene (1.06 g, 2.15 mmol) and $Pd(PPh_3)_4$ (60 mg, 0.05 mmol) were degassed and then heated at 120 °C under constant stirring for 2 h. After 2 h the melt becomes too viscous to be stirred any longer. DMAc (2 mL) was added to the melt and the solution stirred for 22 h at 120 °C. The mixture was allowed to cool to room temperature. Water (150 mL) was added and the red suspension stirred for 1 h. The water was decanted and the residue washed with more water and dried under vacuum. The crude solid was purified by column chromatography (BioRad, BioBeads SX-1) with CH_2Cl_2 (2×) to give pure **2** as a red solid (0.72 g, 40%). ^{1}H NMR (400 MHz, $CDCl_3$) δ 3.37 (s, 6H), 3.55 (m, 4H), 3.66 (m, 28H), 3.80 (m, 4H), 4.42 (m, 4H), 7.09 (m, 6H), 7.12 (d, J = 4.0 Hz, 4H), 7.18 (d, J = 4.0 Hz, 4H), 7.70 (d, J = 4.0 Hz, 4H); ^{13}C NMR (100 MHz, $CDCl_3$) δ 59.00, 64.35, 69.10, 70.47, 70.53, 70.55, 70.59, 70.61, 70.70, 71.88, 123.81, 124.52, 124.58, 124.88, 125.99, 131.34, 134.46, 135.08, 135.64, 136.26, 137.50, 143.77, 161.85.

Mass Spectrometry Studies. Experiments were performed using nanospray ionization on a Bruker BioApex-94e FT-ICR mass spectrometer[30,31] equipped with a shielded 9.4 T magnet (Magnex Scientific Ltd., Abingdon, UK), a 6 cm diameter cylindrical infinity cell, and electrospray ionization source (Analytica of Branford, Branford, CT). Low capillary and skimmer potentials were used to minimize any possibility of the noncovalent bonds of the aggregate being disrupted in the source. An analytical solution of compound **1** (50 μM) and **2** (50 μM) in a solvent mixture (1:1) of THF and aqueous LiCl (10 mM) was prepared by premixing **1** and **2** in THF before further diluting with the aqueous LiCl solution.

Scanning Probe Microscopy Studies. Thin deposits of **1** and **2** were cast on freshly cleaved highly oriented pyrolytic graphite (HOPG) substrates from dilute solutions in toluene (ranging from 10 μM to 1 mM). The solvent was slowly evaporated at room temperature in a solvent-saturated atmosphere. All the AFM images were recorded with a Nanoscope IIIa microscope, operating in tapping mode (25 °C, in air). Microfabricated silicon cantilevers were used with a spring constant of 30 N m^{-1}. The instrument was equipped with the "extender electronics module" to provide simultaneous height and phase cartography. The STM images were obtained in air with mechanically prepared Pt/Ir tips or electrochemically etched W tips. Images of different areas of each sample were recorded. All the images were collected with the maximum available number of pixels (512) in each direction. The nanoscope image-processing software was used for image analysis.

Acknowledgment. We thank Luc Brunsveld and Michel Fransen for providing the penta(ethylene glycol)s. This research is carried out in the framework of the European Commission Training and Mobility of Researchers Networks SELOA (Contract Number ERBFMRX-CT960083) and Laminate (Contract Number). The research of A.P.H.J.S. has been made possible by a fellowship of the Royal Dutch Academy of Arts and Sciences. Research in Mons is supported by the Belgian Federal Government PAI Program (4/11 "*Chimie Supramoléculaire et Catalyse Supramoléculaire*"), and by the EU-Région Wallonne FEDER Objectif 1 Program (NOMAPOL Project). R.L. is maître de Recherches du FNRS (Belgium). Financial support from the Engineering and Physical Sciences Research Council for, inter alia, the FT-ICR is gratefully acknowledged.

JA0113403

(30) Palmblad, M.; Håkansson, K.; Håkansson, P.; Feng, X.; Cooper, H. J.; Giannakopulos, A. E.; Green. P. S.; Derrick, P. J. *Eur. J. Mass Spectrom.* **2000**, *6*, 267.

(31) (a) Heck, A. J. R.; Derrick, P. J. *Anal. Chem.* **1997**, *69*, 3603. (b) Lavanant, H.; Derrick, P. J.; Heck, A. J. R.; Mellon, F. A. *Anal. Biochem.* **1998**, *255*, 74.